Supporting Information

Synthesis of size-controlled boehmite sols: Application in high-performance hydrogen-selective ceramic membranes

Hongsheng Wang, *[a] Sean-Thomas B. Lundin, [a] Kazuhiro Takanabe, [a] and S. Ted Oyama *[a,b,c]

[a.] Department of Chemical System Engineering, School of Engineering, The University of Tokyo, 7-3-1 Hongo, Bunkyo-ku, Tokyo 113-8656, Japan. E-mail: oyama@vt.edu

[b.] Fuzhou University, College of Chemical Engineering, Fuzhou 350116, China.

[c.] Department of Chemical Engineering, Virginia Tech, Blacksburg, VA 24061, United States.

* Corresponding author's email address: oyama@vt.edu; wanghongsheng@whu.edu.cn

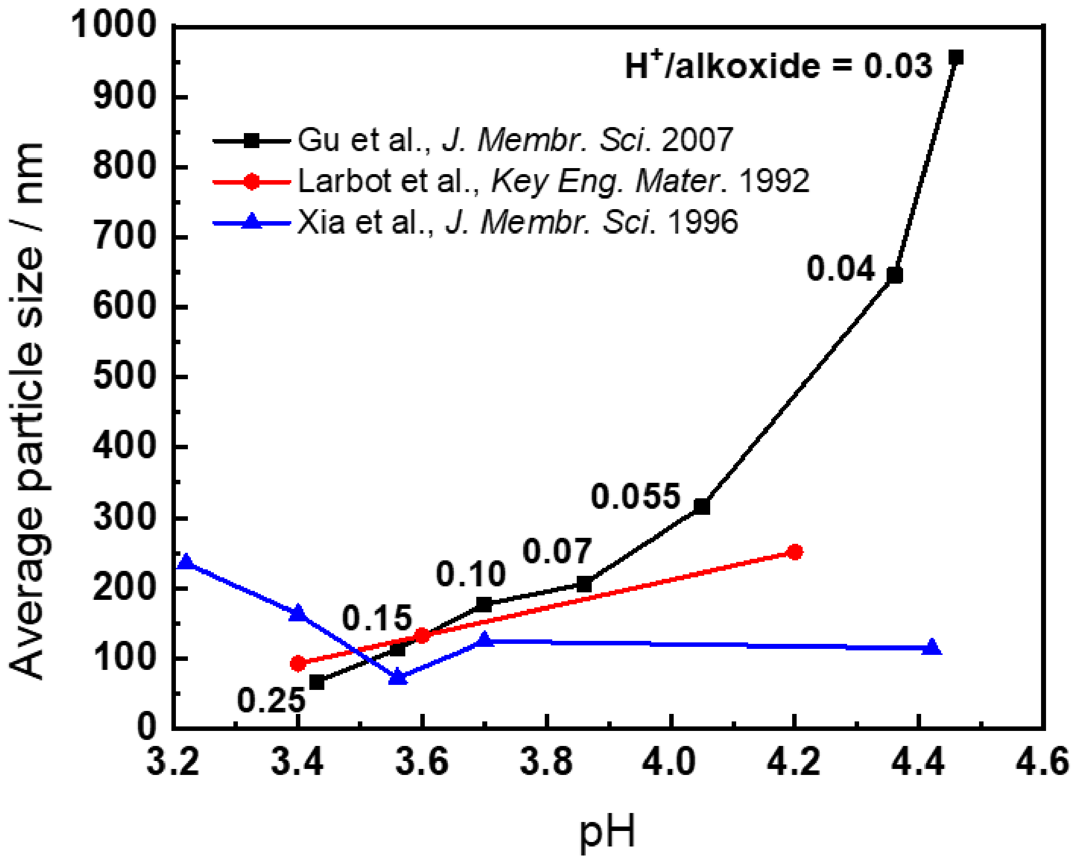

Figure S1. Effect of solution pH on average boehmite sol particle size using HNO_3 measured by DLS in previous studies.

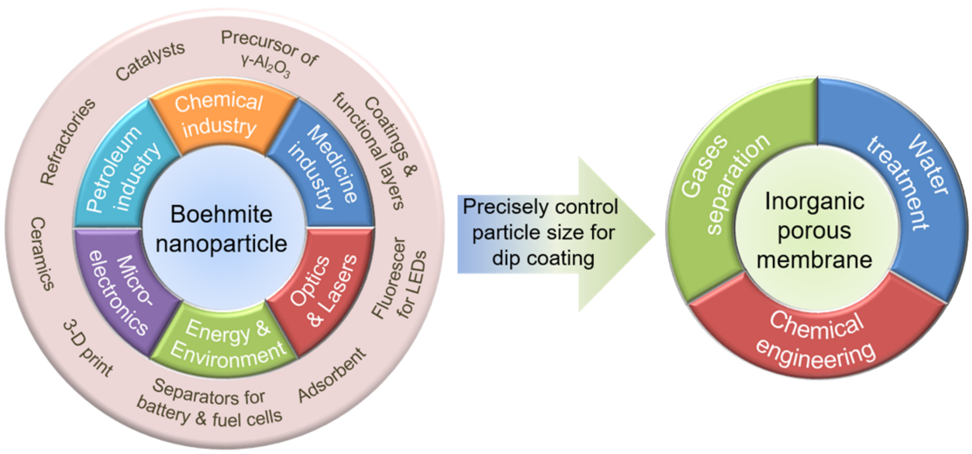

Figure S2. Applications of boehmite nanoparticles and inorganic porous membranes.

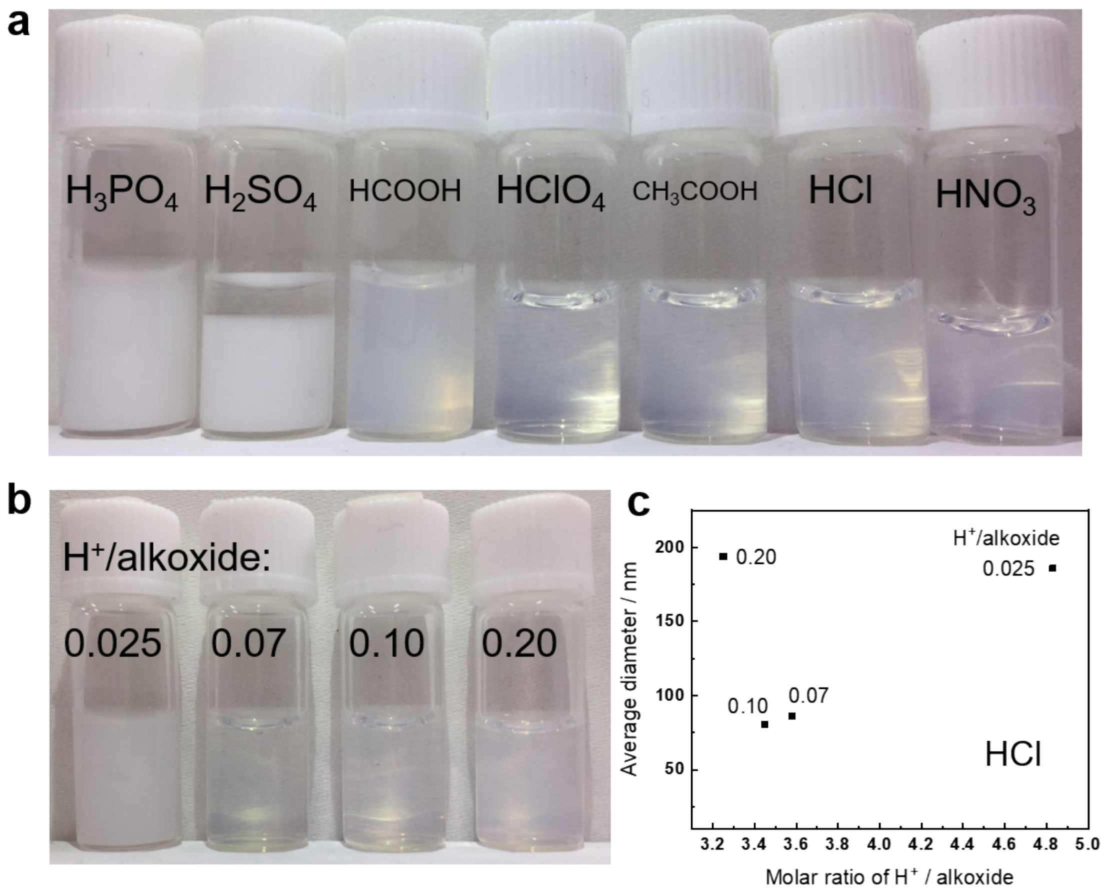

Figure S3. Boehmite sols. a) Photo of boehmite sols synthesized using various acids (H^+/alkoxide = 0.1). b) Photo of boehmite sols using HCl at various H^+/alkoxide ratios. c) Average nanoparticle diameter in the boehmite sols using various HCl concentrations as measured by DLS.

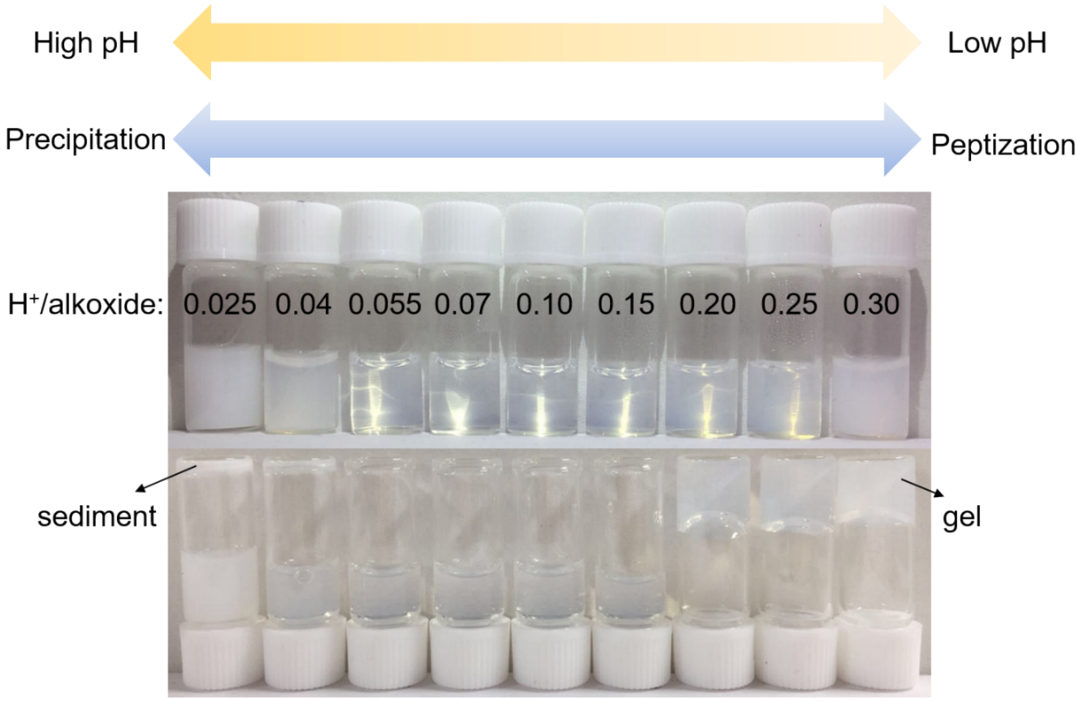

Figure S4. Photos of boehmite sols with different molar ratios of H^+/alkoxide using HNO_3. Top: Containers with sol solutions. Bottom: Inverted containers showing sediment or gel formation.

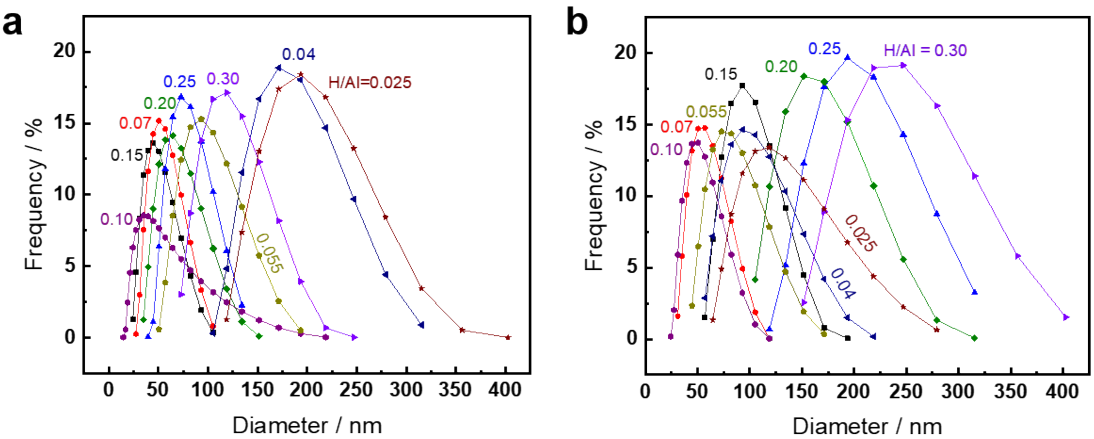

Figure S5. Particle size distributions of boehmite sols produced using different molar ratios of H^+/alkoxide measured by DLS. a) initial size; b) stable size.

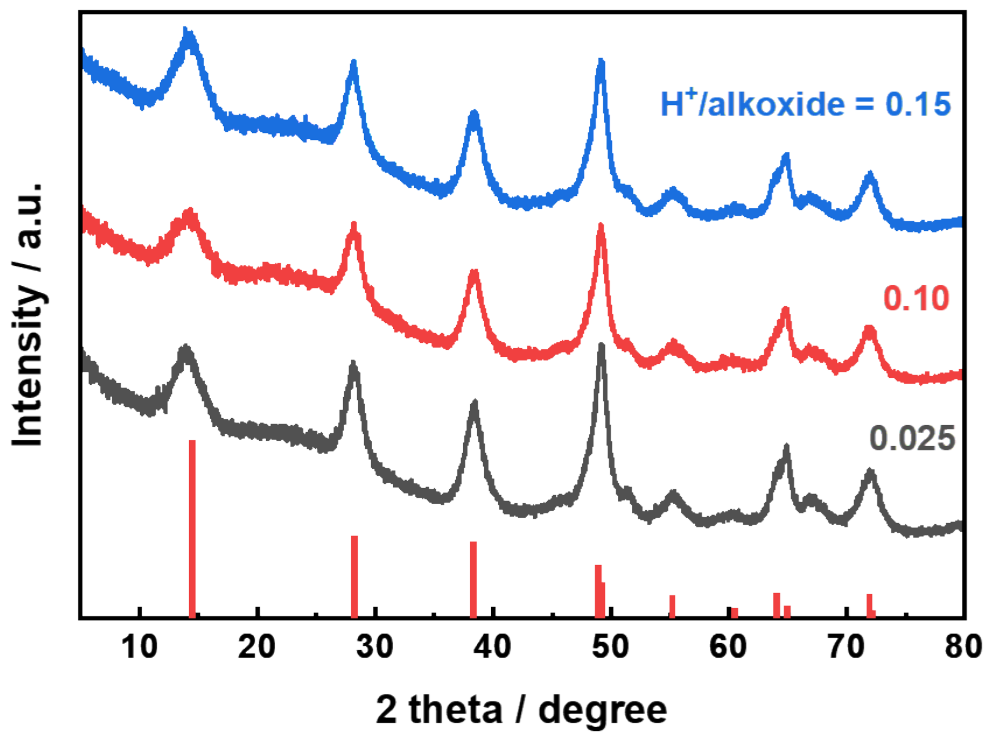

Figure S6. XRD pattern of the boehmite sols dried at 80 °C on quartz plates for the three H^+/alkoxide ratios used in the γ-alumina intermediate layer synthesis step. The signals are compared to boehmite from the American Mineralogist Crystal Structure Database (AMCSD, code: 0014001).

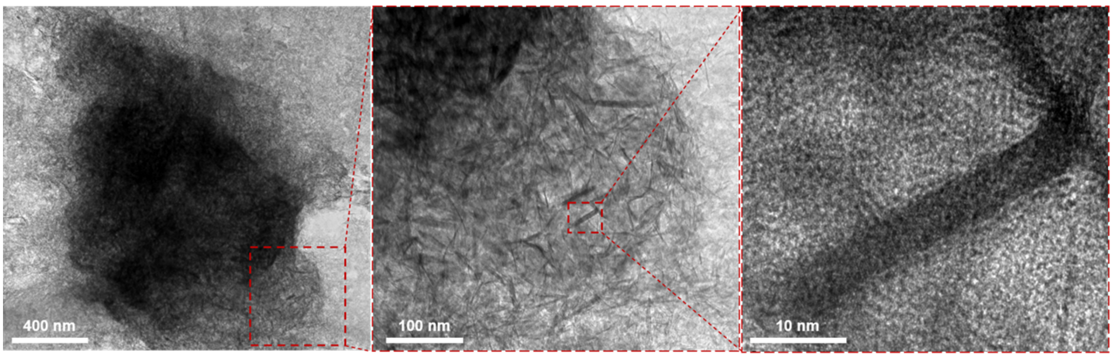

Figure S7. HRTEM of boehmite sample prepared with H^+/alkoxide of 0.025.

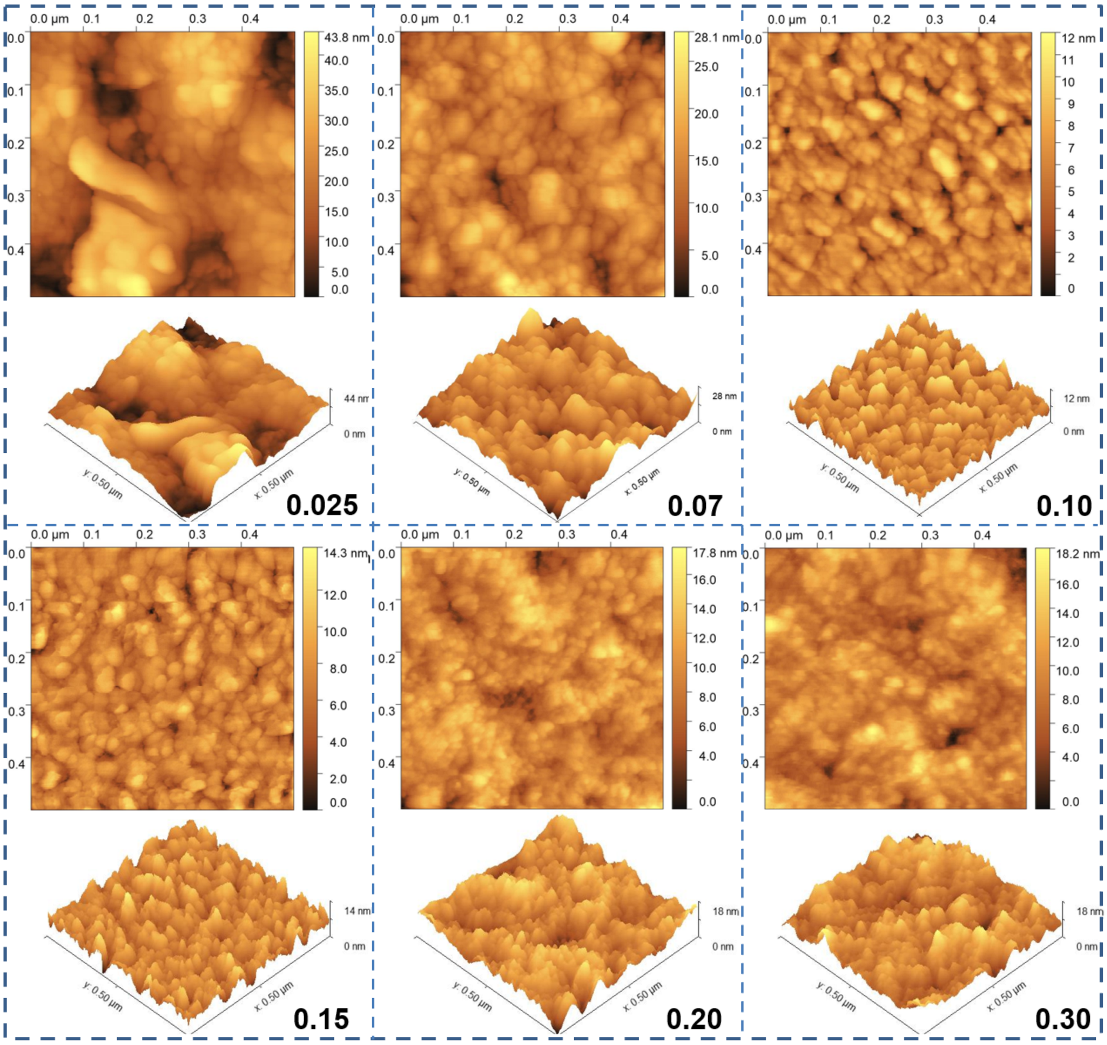

Figure S8. AFM of boehmite particles from different molar ratios of H^+/alkoxide. The boehmite sols were coated on quartz plates and dried in air at room temperature before characterization. The area of the images is 500 × 500 nm.

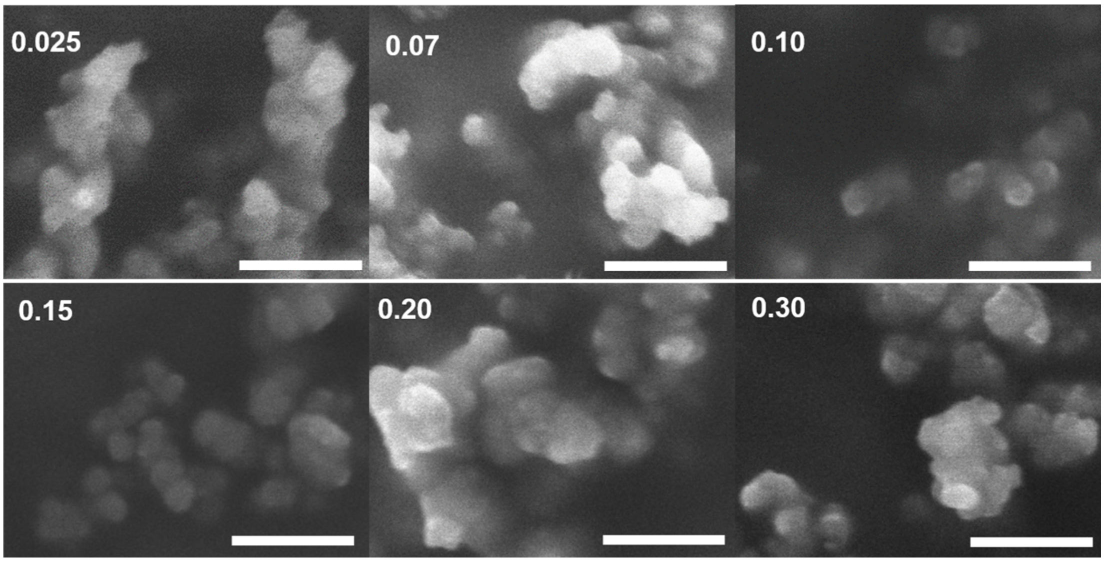

Figure S9. SEM images of the stable boehmite sols produced from different molar ratios of H^+/alkoxide. The boehmite sols were dried in air at room temperature before characterization. Scale bar: 250 nm.

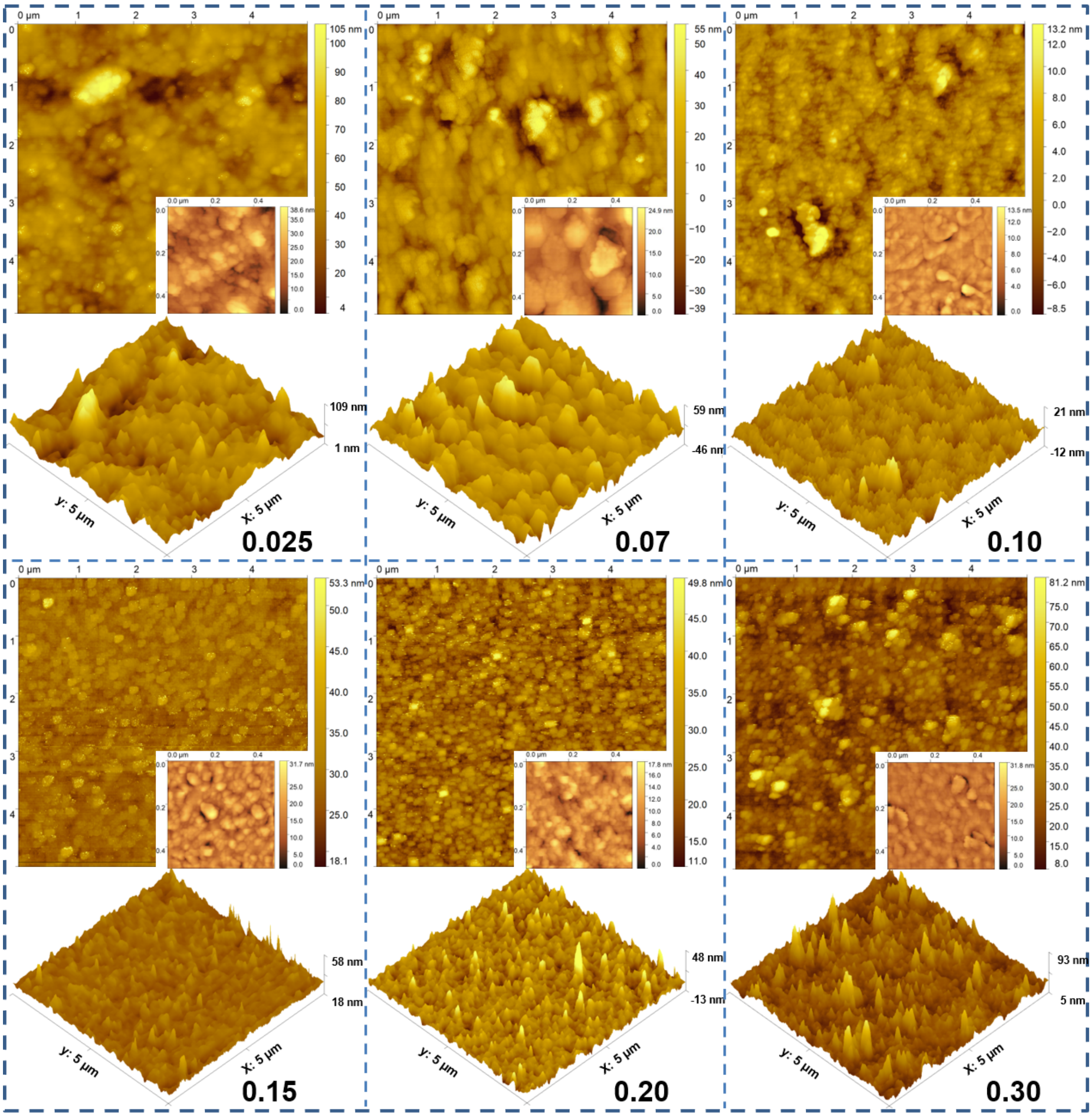

Figure S10. AFM images of the γ-alumina layers produced using different molar ratios of H^+/alkoxide after dip-coating and calcining at 650 °C on quartz plates. The area of the primary images is 5 μm × 5 μm, and the inserted subfigures (bottom right corner) has an area of 500 nm × 500 nm.

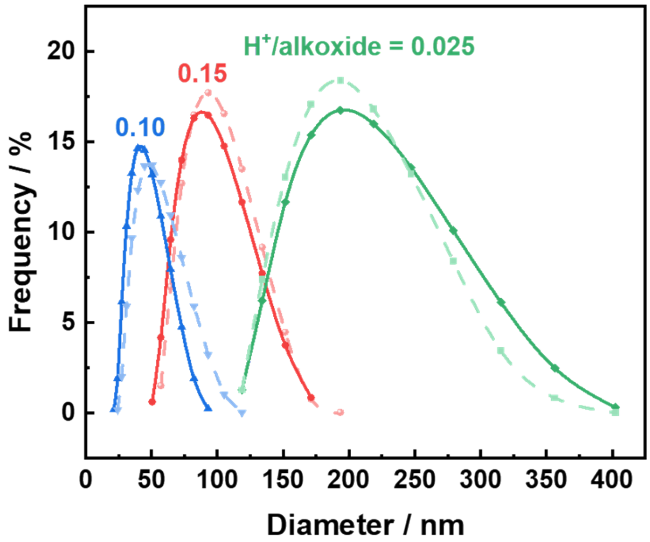

Figure S11. DLS measured particle size distributions for the optimized sols selected for membrane preparation. Solid lines indicate boehmite particles in acid solution without PVA, and dashed line indicates result after PVA addition.

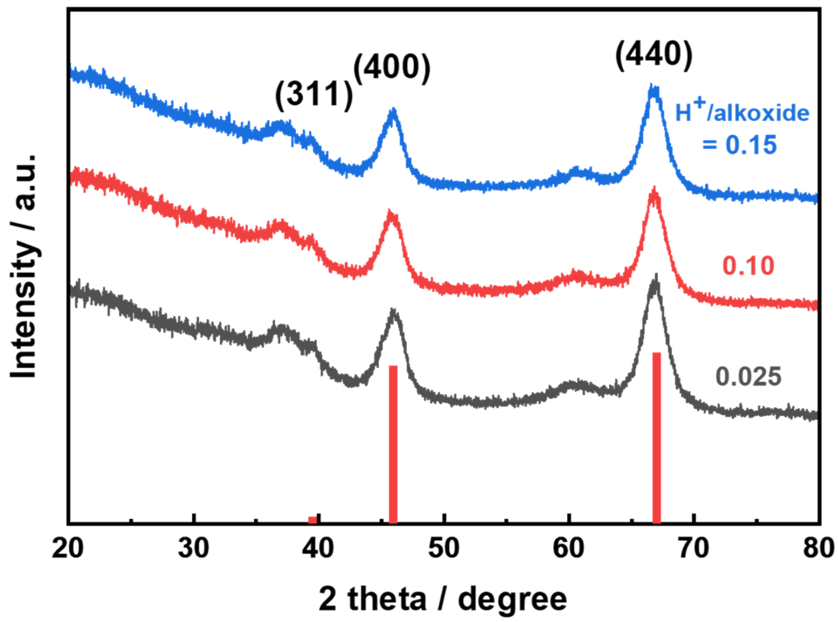

Figure S12. XRD pattern for the γ-alumina powder produced from each boehmite sol after calcination at 650 °C on quartz plates. The signals are compared to γ-alumina from the American Mineralogist Crystal Structure Database (AMCSD, code: 0010553).

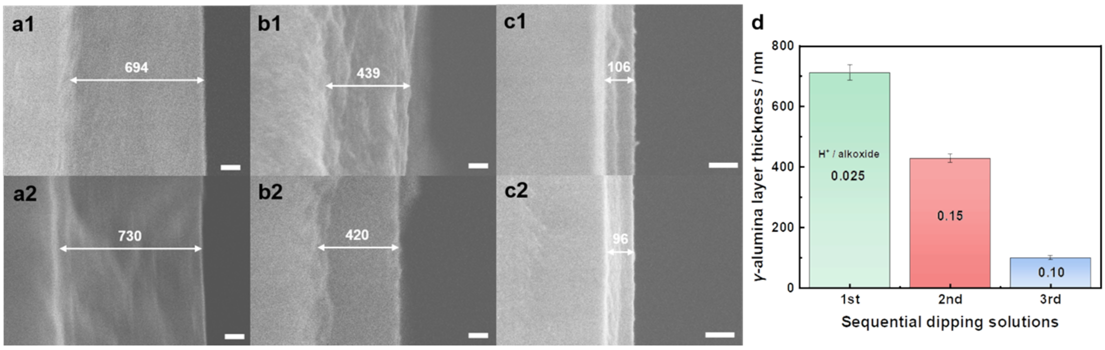

Figure S13. Thickness evaluation for each dipping solution after calcination at 650 °C on quartz plates using SEM cross-sectional images. a1) and a2): 1st dipping solution; b1) and b2): 2nd dipping solution; c1) and c2) 3rd dipping solution; d) average particle size. Scale bar: 100 nm.

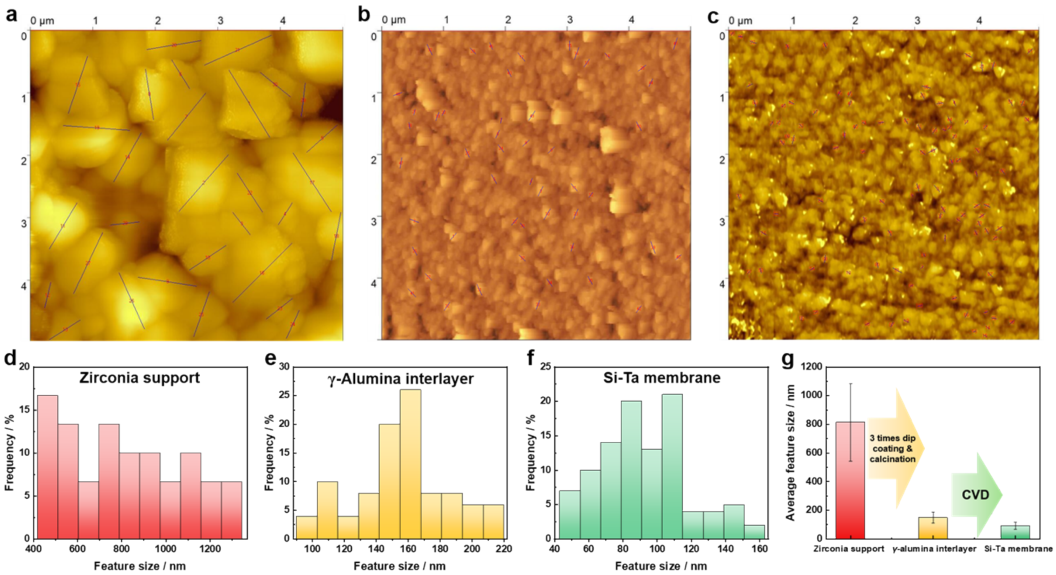

Figure S14. Feature size estimation using AFM images a) bare zirconia support, b) resultant γ-alumina intermediate layer after the dip-coat and calcination process, and c) Si-Ta composite membrane after CVD process (same images shown in Figure 4, sans particle annotations). The feature size distributions are respectively shown in d) - f), and the average feature size is exhibited in e). 30 features, 50 features, and 100 features were randomly selected for the size estimation in a), b), and c), respectively.

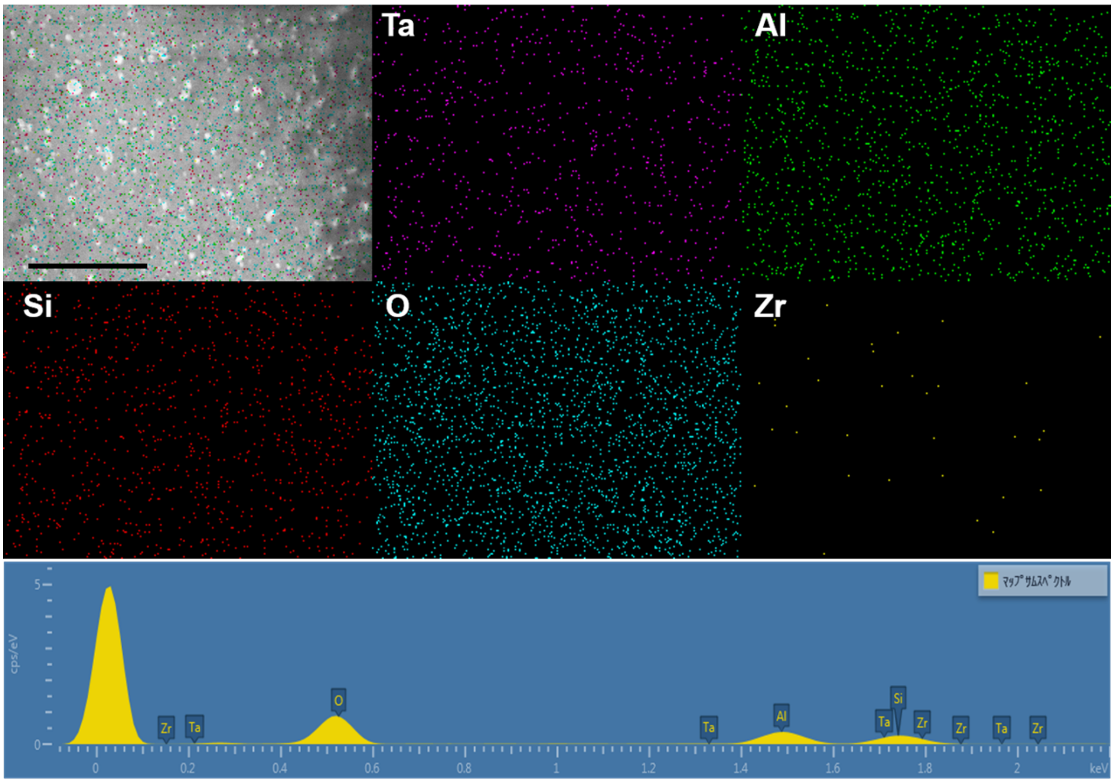

Figure S15. SEM and EDS images of the composite Si-Ta membrane. Scale bar: 500 nm.

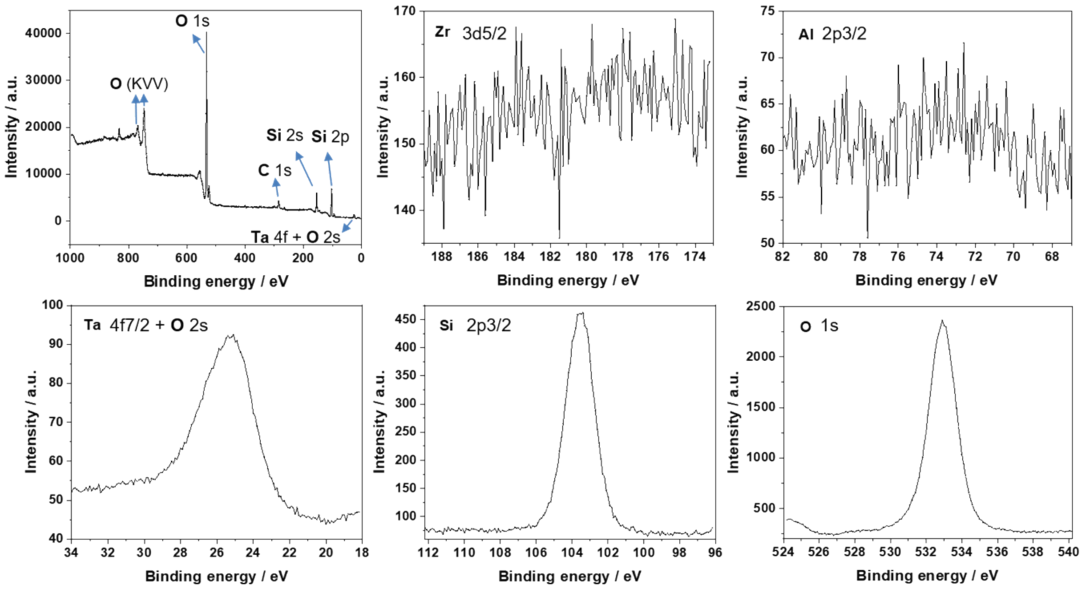

Figure S16. XPS spectra of the Si-Ta composite membrane surface.

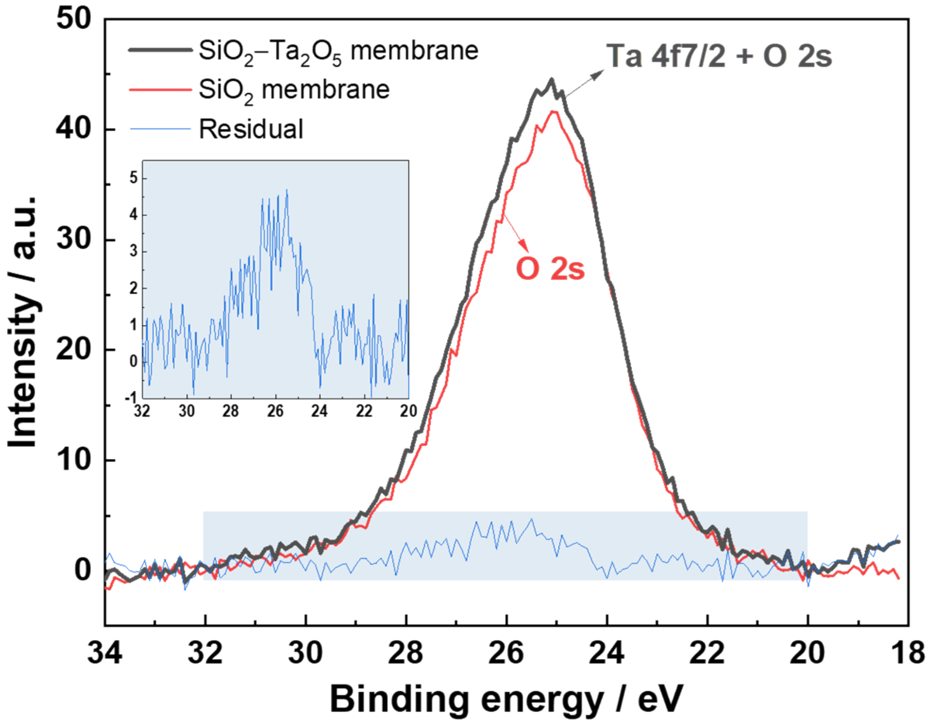

Figure S17. Analysis of the XPS spectra of Ta on the Si-Ta composite membrane surface. The residual (blue line) is the difference between the XPS spectra of the Si-Ta membrane (black line) and that of a silica control membrane synthesized without tantalum (red line).

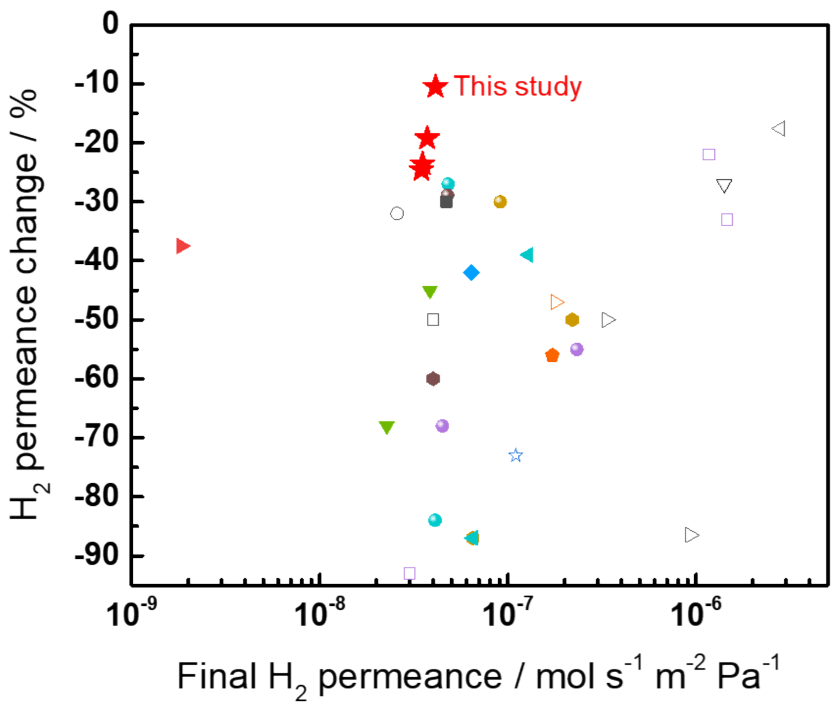

Figure S18. Comparison with literature reports of H_2 permeance change after hydrothermal stability test versus final H_2 permeance. Open symbol: sol-gel method; filed symbol: CVD method.

Table S1. Boehmite nanoparticle size from DLS using several acids.

	H_3PO_4	H_2SO_4	HCl	$HClO_4$	CH_3COOH	HCOOH	HNO_3
H^+/alkoxide	0.1	0.1	0.1	0.1	0.1	0.1	0.1
Size / nm	870	-	81	58	81	80	53

Table S2. XRD crystal domain of boehmite sol and γ-alumina particle from Scherrer analysis.

Ratio of H^+/alkoxide	Crystal domain / nm	
	XRD	
	Boehmite	γ-Al_2O_3
0.025	3.4	5.5
0.07	-	-
0.10	3.2	4.1
0.15	3.2	5.6
0.20	-	-
0.30	-	-

Table S3. Summary of particle size measurement. DLS and SEM represent particle sizes of boehmite sols, and AFM provides the results from both boehmite sol and γ-alumina after calcination at 650 ºC.

Ratio of H^+/alkoxide	Particle size / nm			
	DLS	SEM	AFM	
	Boehmite	Boehmite	Boehmite	γ-Al_2O_3
0.025	210	56	31	33
0.07	65	53	23	27
0.10	51	47	22	22
0.15	90	49	20	23
0.20	145	50	17	25
0.30	220	53	16	27

Table S4. Surface roughness calculation of boehmite sol and γ-alumina particle from R_{3Z} values in AFM characterization. γ-Al_2O_3 without PVA is calculated from the calcination of boehmite sol, and γ-Al_2O_3 with PVA is the result from calcination of dip coating solution, which is prepared by boehmite sol mixed with PVA. The calcination temperature is 650 ºC.

Ratio of H^+/alkoxide	Surface roughness / nm		
	AFM		
	Boehmite	γ-Al_2O_3 without PVA	γ-Al_2O_3 with PVA
0.025	37	41	44
0.07	20	24	-
0.10	16	11	15
0.15	16	14	20
0.20	14	15	-
0.30	12	23	-

Table S5. EDS elemental distribution on the surface of Si-Ta and pure silica composite membranes collected at 15 kV accelerating voltage.

		O	**Al**	**Si**	**Ta**	**Zr**	**Molar ratio of Ta/Si**
SiO_2–Ta_2O_5 membrane	wt%	64.6	18.5	15.0	1.8	0	1.9×10^{-2}
	σ	2.9	1.1	1.3	3.9	0	
Pure SiO_2 membrane	wt%	63.3	20.5	16.2	0	0	0
	σ	1.0	0.7	0.9	0	0	

Table S6. XPS and ICP elemental distributions of the Si-Ta membrane.

wt%	**O**	**Al**	**Si**	**Ta**	**Zr**	**Molar ratio of Ta/Si**
ICP	49.2	46.4	1.86	0.07	2.41	5.8×10^{-3}
XPS	50.0	-	49.3	0.71	-	2.2×10^{-3}

Table S7. Summary of previous reports on silica-based porous membranes.

Membrane material	Precursor	Method	Support material	Support pore size / nm	Membrane synthesis temperature / °C	Test temperature / °C	Membrane thickness / µm	H_2 permeance / mol m^{-2} s^{-1} Pa^{-1}	Selectivity			Symbols in Fig. 5	Ref.
									H_2/N_2	H_2/CH_4	H_2/O_2		
SiO_2	SiH_4+O_2	CVD	Vycor glass	4	450	600	0.1	1.40×10^{-8}	3000	-	-		[1]
SiO_2	TEOS+O_2	CVD	Porous glass	4	200	200	-	5.00×10^{-9}	11	-	6 (He/O_2)		[2]
SiO_2	SiH_4+O_2	CVD	Vycor glass	4	450	600	0.1	4.05×10^{-10}	300	-	-		[3]
SiO_2	$SiCl_4+H_2O$	CVD	Vycor glass	4	800	450	-	2.2×10^{-8}	7000	-	-		[4]
SiO_2	TPS+O_2	CVD	Vycor glass	4	750	750	3	9.00×10^{-9}	250	-	-		[5]
								1.83×10^{-8}	146	-	-		
SiO_2	$Cl_3SiOSiCl_3+H_2O$	CVD	Vycor glass	4	700	700	-	2.20×10^{-8}	1360	-	-		[6]
	$Cl_3SiOSiCl_2OSiCl_3+H_2O$							3.29×10^{-8}	813	-	-		
SiO_2	TEOS+O_2	CVD	Vycor glass	4	300	600	-	1.73×10^{-8}	880	-	-		[7]
	$SiCl_4+H_2O$							9.95×10^{-9}	2040	-	-		
SiO_2	TEOS	CVD	α-Al_2O_3	110-180	600	600	0.05-0.1	2.00×10^{-8}	1000	-	-		[8]
					500			3.00×10^{-7}	100	-	-		
SiO_2	$SiCl_4+H_2O$	CVD	Vycor glass	4	750	600	0.04	2.43×10^{-8}	471	-	-		[9]
								8.84×10^{-9}	1200	-	-		
SiO_2	TEOS+O_2	CVD	γ-Al_2O_3	4	600	600	1.5	1.03×10^{-9}	28	-	-		[10]
SiO_2	TEOS+O_2	CVD	γ-Al_2O_3	4	300	600	1.5-3	4.88×10^{-9}	36	-	-		[11]
								8.07×10^{-9}	20	-	-		

SiO_2	TEOS	Sol-gel	α-Al_2O_3	160	400	200	0.06-0.12	2.86×10^{-6}	31.8	77.3	11.4		[12]
SiO_2+TiO_2	TEOS+TIP	Sol-gel	α-Al_2O_3	160	400	150	0.06-0.15	~1×10^{-7}	-	200	-		[13]
						200			-	160	-		
SiO_2	$SiCl_4$+H_2O	CVD	Vycor glass	4	700	700	3-10	1.28×10^{-7}	424	-	-		[14]
								7.66×10^{-8}	2476	-	-		
					700	600		9.80×10^{-8}	359	-	-		
								5.16×10^{-8}	4667	-	-		
					800	800		1.22×10^{-7}	1269	-	-		
								8.55×10^{-8}	3515	-	-		
					800	600		2.06×10^{-8}	739	-	-		
								2.06×10^{-8}	1556	-	-		
SiO_2	$SiCl_4$+H_2O	CVD	Vycor glass	4	600	450	-	6.28×10^{-8}	1112	-	-		[15]
						600		5.70×10^{-8}	989	-	-		
						700		5.41×10^{-8}	625	-	-		
			Vycor glass with carbon barrier			450		2.09×10^{-7}	4819	-	-		
						600		4.15×10^{-7}	8190	-	-		
						700		6.19×10^{-7}	7776	-	-		
SiO_2	TEOS	CVD	α-Al_2O_3	150	650	600	0.5	1.20×10^{-7}	3.74	-	-		[16]
SiO_2	DES+O_2	CVD	Vycor glass	4	450	450	-	1.60×10^{-8}	800	-	-		[17]
SiO_2	TEOS	CVD	α-Al_2O_3	150	600-700	600	0.1	3.00×10^{-7}	100	-	-		[18]
								6.50×10^{-8}	3250	-	-		
SiO_2	TEOS	CVD	α-Al_2O_3	150	600	600	-	2.25×10^{-8}	>2250	-	-		[19]
SiO_2+Al_2O_3	TEOS, ATSB+O_2	CVD	-	4	400	400	0.13	1.99×10^{-8}	40	-	-		[20]
SiO_2	TEOS	CVD	α-Al_2O_3	110-180	500-650	600	-	2.20×10^{-8}	43	-	-		[21]

	PTES				500	200	-	5.70×10^{-8}	33	-	-		
	DPDES				500	200	0.2	5.00×10^{-7}	64	-	-		
SiO_2	TEOS	Sol-gel	α-Al_2O_3	160	400	200	0.03	2.00×10^{-6}	-	500	-	◇	[22]
								5.00×10^{-7}	135	4000	-		
SiO_2	$SiAc_4+O_2$	CVI	α-Al_2O_3	80	275	250	-	4.00×10^{-7}	43	-	-	◀	[23]
SiO_2	TEOS	Sol-gel	α-Al_2O_3	160	400	200	0.03	1.85×10^{-6}	64	561	20	▷	[24]
						25		7.33×10^{-7}	59	844	19		
SiO_2	TEOS	CVD	Vycor glass	150	600	20-600	-	1.99×10^{-8}	2013	-	-	⬢	[25]
								3.99×10^{-9}	400	-	-		
								9.91×10^{-9}	1008	-	-		
SiO_2	TEOS	CVD	α-Al_2O_3	110-180	900	600	0.1	1.05×10^{-8}	107	-	-	●	[26]
SiO_2	TEOS	CVD	α-Al_2O_3	50	600	600	0.1-0.2	6.00×10^{-9}	160	-	-	★	[27]
SiO_2	TEOS+MTES	Sol-gel	α-Al_2O_3	160	400	100	0.06	2.27×10^{-6}	8.25	8.53	5.83	□	[28]
SiO_2	$TEOS+O_2$	CVD	Vycor glass	4	600	600	-	1.80×10^{-8}	-	23000-27000	-	●	[29]
								2.50×10^{-8}	10000	-	-		
SiO_2	$TEOS+O_3+O_2$	CVD	Vycor glass	4	200	40	-	2.00×10^{-8}	670	-	-	▼	[30]
								2.95×10^{-8}	355	405	34		
SiO_2	TEOS	CVD	α-Al_2O_3	10	600	600	<1	7.69×10^{-9}	135	-	-	⬟	[31]
SiO_2	TEOS	Sol-gel	γ-Al_2O_3	5	300-500	80	0.03	3.35×10^{-7}	317	1270	-	△	[32]
SiO_2	TEOS	CVD	α-Al_2O_3	150	600	450	-	1.59×10^{-7}	20	14	-	★	[33]
SiO_2	$TEOS+TIPT+O_2$	CVD	Vycor glass	4	600	600	-	1.40×10^{-8}	1000	-	-	●	[34]
SiO_2	$TEOS+O_2$	CVD	Porous glass	2	450	200	-	4.30×10^{-9}	100	-	-	■	[35]
SiO_2	TEOS	CVD	α-Al_2O_3	110-180	600	600	-	4.00×10^{-7}	150	-	-	■	[36]

SiO_2	TEOS+MOTMS	Sol-gel	α-Al_2O_3	150	600	100	-	2.40×10^{-7}	78	235	-		[37]
						200		4.04×10^{-7}	90	185	-		
						300		6.80×10^{-7}	30	115	-		
SiO_2	TEOS	CVD	α-Al_2O_3	110-180	600	450	0.15	1.00×10^{-7}	12	19	-		[38]
SiO_2+ZrO_2	TEOS+ZTBO	Sol-gel	α-Al_2O_3	1000	500	-	<1	3.40×10^{-7}	193	-	-		[39]
SiO_2	TEOS	Sol-gel	α-Al_2O_3	1000	500	300	1	1.30×10^{-6}	-	150	-		[40]
SiO_2	TEOS	Sol-gel	α-Al_2O_3	-	360-570	150	-	3.84×10^{-6}	7	7	5		[41]
						200		1.82×10^{-6}	16	-	45		
SiO_2+ZrO_2	TEOS+ZTBO	Sol-gel	α-Al_2O_3	1	570	500	-	1.58×10^{-7}	220	-	-		[42]
SiO_2	TMOS	CVD	Vycor glass	3.6	600	600	0.01	1.00×10^{-8}	10769	20000	-		[43]
SiO_2+NiO	TEOS+ $Ni(NO_3)_2$	Sol-gel	α-Al_2O_3	1000	180-190	200	-	6.70×10^{-7}	-	350	-		[44]
SiO_2	TEOS	Sol-gel	α-Al_2O_3	500-1000	500	200	0.25-0.30	1.50×10^{-6}	18	-	-		[45]
SiO_2	TEOS	CVD	α-Al_2O_3	100	600	600	-	1.80×10^{-8}	63.7	-	-		[46]
SiO_2	TEOS+MOTMS	Sol-gel	α-Al_2O_3	150	600	100	-	1.58×10^{-7}	39	88			[47]
SiO_2	TEOS	CVD	α-Al_2O_3	5	600	600	0.02-0.03	1.00×10^{-7}	1000	-	-		[48]
								1.20×10^{-7}	-	2800	-		
SiO_2	TEOS	Sol-gel	α-Al_2O_3	80	500	200	0.02-0.05	1.05×10^{-6}	15	-	-		[49]
SiO_2	TEOS	Sol-gel	α-Al_2O_3	1000	500	500	<1	2.60×10^{-7}	87	-	-		[50]
SiO_2	TEOS	CVD	α-Al_2O_3	5	600	600	-	3.00×10^{-7}	-	300	-		[51]
SiO_2	TMOS+O_2/O_3	CVD	α-Al_2O_3	100	600	600	-	1.50×10^{-7}	1000	-	-		[52]
SiO_2	TEOS	Sol-gel	α-Al_2O_3	300	600	600	<0.02	2.38×10^{-6}	102	-	-		[53]
Ni/SiO_2	TEOS+$Ni(NO_3)_2$	Sol-gel	α-Al_2O_3	1000	550	500	0.5	1.03×10^{-6}	160	-	-		[54]
SiO_2	TMOS+O_2	CVD	α-Al_2O_3	-	600	500	0.02	6.70×10^{-8}	145	-	-		[55]

					500	500		1.59×10^{-7}	710	-	-		
						300		9.05×10^{-8}	2640	-	-		
						100		3.07×10^{-8}	5950	-	-		
SiO_2	TEOS	CVD	α-Al_2O_3	5	650	600	-	1.00×10^{-7}	-	700	-		[56]
SiO_2	TEOS+O_2	CVD	α-Al_2O_3	100	600	600	-	4.38×10^{-8}	2900	2400	-		[57]
SiO_2	TEOS	CVD	α-Al_2O_3	100	600	600	0.02-0.03	5.00×10^{-7}	5930	5900	-		[58]
SiO_2	TMOS+O_2	CVD	α-Al_2O_3	100	600	600	-	6.43×10^{-7}	2300	-	-		[59]
SiO_2	TMMOS	CVD	α-Al_2O_3	100	600	600	-	3.00×10^{-7}	211	-	-		[60]
	PrTMOS				500	500		1.10×10^{-7}	75	-	-		
	TMOS							9.10×10^{-8}	540	-	-		
	PhTMOS							1.30×10^{-7}	35	-	-		
SiO_2	TEOS+O_2	CVD	α-Al_2O_3	150	600	300	-	5.00×10^{-8}	-	24000	-		[61]
SiO_2	TEOS	Sol-gel	Stainless steel (SUS 316)	500	600	291	1	4.32×10^{-9}	22	-	-		[62]
SiO_2	TMOS+O_2	CVD	α-Al_2O_3	150	600	500	2.3	2.98×10^{-8}	12200	-	-		[63]
SiO_2	TMOS+O_2	CVD	α-Al_2O_3	100	600	600	-	1.40×10^{-7}	10000	-	-		[64]
SiO_2	DMDPS+O_2	CVD	α-Al_2O_3	100	600	300	-	1.50×10^{-6}	158	-	-		[65]
	PTMS+O_2							1.88×10^{-7}	1010	-	-		
SiO_2	TEOS	CVD	α-Al_2O_3	-	400	400	-	7.00×10^{-7}	57	-	-		[66]
SiO_2+Co_3O_4	TEOS+$Co(NO_3)_2$	Sol-gel	α-Al_2O_3	1000	600	500	-	4.00×10^{-7}	730	-	-		[67]
SiO_2+Co_3O_4	TEOS+$Co(NO_3)_2$	Sol-gel	α-Al_2O_3	500-1000	500	200	-	3.40×10^{-8}	275	-	-		[68]
SiO_2+Al_2O_3	TEOS+ATSB	CVD	α-Al_2O_3	100	600	600	0.03-0.04	1.60×10^{-7}	-	940	-		[69]
SiO_2+Nb_2O_5	TEOS+NPB	Sol-gel	α-Al_2O_3	-	500	200	0.03	6.30×10^{-7}	150	560	-		[70]

Ni/SiO_2	TEOS+$Ni(NO_3)_2$	Sol-gel	α-Al_2O_3	1000	550	500	<1	2.41×10^{-7}	502	-	-	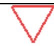	[71]
SiO_2+TiO_2	TEOS+TIP	CVD	α-Al_2O_3	5	600	600	0.01-0.02	2.10×10^{-7}	-	50	-		[72]
SiO_2	BTESE	Sol-gel	α-Al_2O_3	1000	300	200	-	2.00×10^{-5}	8	-	-		[73]
								8.00×10^{-6}	9	-	-		
SiO_2	TEOS+O_2	CVI	α-Al_2O_3	200	300	300	-	7.10×10^{-8}	91	-	-		[74]
SiO_2	BTESE	Sol-gel	α-Al_2O_3	1000	300	200	<0.04	7.90×10^{-6}	8.87	-	-	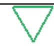	[75]
SiO_2	TEOS+O_3	CVI	α-Al_2O_3	80	250	250	-	1.53×10^{-8}	19.4	-	-		[76]
SiO_2+Al_2O_3	TEOS+ATSB	CVD	α-Al_2O_3	5	600	350	0.03	6.80×10^{-8}	-	350	-		[77]
SiO_2	TEOS	Sol-gel	α-Al_2O_3	-	600	250	0.03	6.00×10^{-7}	-	660	-		[78]
								1.00×10^{-6}	180	490	-		
SiO_2	HMDSO+O_2	PECVD	α-Al_2O_3	4	25	50	1-2	1.60×10^{-9}	1330	-	-		[79]
SiO_2+Co_3O_4	TEOS+ $Co(NO_3)_2$	Sol-gel	α-Al_2O_3	1000	600	500	0.05	1.80×10^{-7}	730	-	-		[80]
SiO_2	HEDS	Sol-gel	α-Al_2O_3	100-150	550	200	0.3-0.4	8.86×10^{-7}	20	-	-		[81]
SiO_2+Al_2O_3	TEOS+ATSB	CVD	α-Al_2O_3	500	600	800	0.08-0.1	6.30×10^{-7}	203	573	-		[82]
SiO_2	TEOS	Sol-gel	α-Al_2O_3	-	630	500	-	1.75×10^{-7}	890		-	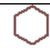	[83]
SiO_2	TEOS+PTES	CVD	α-Al_2O_3	5	600	600	0.25	2.10×10^{-7}	-	89	-		[84]
								1.00×10^{-6}	-	55	-		
SiO_2	BTESE	Sol-gel	α-Al_2O_3	1000	350	200	<1	4.74×10^{-6}	8.13	10.8	-		[85]
	BTESM							4.51×10^{-6}	28.1	47.3	10.8		
SiO_2	BTESM	Sol-gel	α-Al_2O_3	1000	200	200	-	1.45×10^{-7}	-	430	-		[86]
					600			2.95×10^{-6}	20	26	-		
SiO_2	TMOS	CVD	α-Al_2O_3	4	650	650	-	4.00×10^{-8}	1265	-	-		[87]
SiO_2	DMDMOS	CVD	α-Al_2O_3	100	500	600	-	9.00×10^{-7}	920	-	-		[88]
	TMOS							1.80×10^{-7}	609	-	-		
	MTMOS							2.90×10^{-7}	586	-	-		

	TMMOS							5.40×10^{-7}	512	-	-		
SiO_2	PrTMOS	CVD	γ-Al_2O_3	4	240	240	-	2.50×10^{-7}	250	-	-	▲	[89]
	HTMOS				360	360		3.00×10^{-7}	15	-	-		
SiO_2	BTESE	Sol-gel	α-Al_2O_3	1000	550	200	-	9.50×10^{-7}	22.2	-	-	▽	[90]
	BTESEthy							1.61×10^{-6}	39.5	-	-		
	BTESA							2.68×10^{-6}	10.3	-	-		
SiO_2	TEOS	Sol-gel	α-Al_2O_3	570	600	200	-	1.50×10^{-7}	31.3	-	-	◇	[91]
SiO_2	TEOS	Sol-gel	α-Al_2O_3	570	600	200	-	1.10×10^{-6}	26.2	-	-	⬡	[92]
SiO_2	OMDSO	PECVD	α-Al_2O_3	150	Room temperature	Room temperature	-	2.00×10^{-8}	10	-	-	●	[93]
	TMMOS							1.13×10^{-8}	11	-	-		
	MTMOS							7.60×10^{-9}	17	-	-		
SiO_2	TEOS+PTMS	CVD	α-Al_2O_3	5	120	120	0.03	2.50×10^{-7}	64.1	43.1	-	◀	[94]
	TEOS+APTMS	CVD	α-Al_2O_3					3.00×10^{-7}	273	714	-		
	TEOS+MAPTMS	CVD	α-Al_2O_3					5.80×10^{-7}	93.5	264	-		
SiO_2	TPMS	CVD	α-Al_2O_3	150	600	300	-	1.20×10^{-6}	8	-	-	▶	[95]
	DPDMS							7.60×10^{-7}	14	-	-		
SiO_2+ZrO_2	TEOS+ZTB	CVD	α-Al_2O_3	60	650	650	0.03	3.80×10^{-7}	1400	3700	-	⬟	[96]
SiO_2	HTMOS	CVD	α-Al_2O_3	4	450	450	-	1.53×10^{-7}	575	-	-	▲	[97]
$SiO_2+Al_2O_3$	TEOS+ATSB	CVD	α-Al_2O_3	5	650	650	0.03	4.90×10^{-7}	500	-	-	▼	[98]
								8.20×10^{-8}	-	108	-		
SiO_2	BTESE	Sol-gel	α-Al_2O_3	1000	300	200	-	4.70×10^{-7}	40	60	-	○	[99]
SiO_2	VTES	CVD	α-Al_2O_3	60	600	300	-	2.70×10^{-7}	190	207	-	▲	[100]
SiO_2	VTES	CVD	α-Al_2O_3	60	600	600	0.2	5.40×10^{-7}	170	480	-	●	[101]
F-induced SiO_2	TEFS	Sol-gel	α-Al_2O_3	500	350	300	-	1.92×10^{-6}	10.5	12	-	▽	[102]

					750			1.52×10^{-6}	15	21	-		
SiO_2	BTESE	Sol-gel	α-Al_2O_3	1000	300	200	-	2.85×10^{-7}	105	150	-	○	[103]
SiO_2	TRIES	Sol-gel	α-Al_2O_3	500	550	300	-	2.34×10^{-7}	220	590	-	□	[104]
SiO_2	POSS	Sol-gel	α-Al_2O_3	1000	500	200	-	5.15×10^{-7}	42	55	-	○	[105]
SiO_2	TEOS+TMMOS	CVD	α-Al_2O_3	60	650	300	0.03	8.30×10^{-7}	90	140	-	◆	[106]
								1.10×10^{-6}	53	-	-		
								2.41×10^{-8}	1220	15800	-		
SiO_2	HMDSO	AP-PECVD	α-Al_2O_3	2000	50	50	0.013	1.22×10^{-7}	15	8.5	-	⬢	[107]
					100			5.45×10^{-7}	17.5	17	-		
					200			2.80×10^{-6}	7	6.5	-		
SiO_2+ZrO_2	TEOS+ZTB	Sol-gel	α-Al_2O_3	1200	250	200	-	1.80×10^{-7}	23	47	-	□	[108]
						50		4.50×10^{-8}	31	100	-		
SiO_2	BTESP	Sol-gel	α-Al_2O_3	1000	350	200	-	9.80×10^{-7}	33	50	-	○	[109]
SiO_2	BTESA+APTES	Sol-gel	α-Al_2O_3	1000	250	200	500	1.40×10^{-6}	35.5	57.5	-	⬠	[110]
								3.35×10^{-7}	53	73	-		
SiO_2+ZrO_2	MAPTMS+ZTB	Sol-gel	α-Al_2O_3	1200	250	200	<400	2.05×10^{-7}	31.5	28	-	⬡	[111]
SiO_2	BTESE	Sol-gel	α-Al_2O_3	1000	150	150	-	1.92×10^{-7}	92	96	-	☆	[112]
								7.35×10^{-8}	145	263	-		
SiO_2+Ni	BTPA+$Ni(NO_3)_2$	Sol-gel	α-Al_2O_3	1000	250	200	13-50	4.60×10^{-6}	12	8	-	◇	[113]
SiO_2+Cu	BTPA+$Cu(NO_3)_2$							4.30×10^{-6}	25	23	-		
SiO_2+Ag	BTPA+$AgNO_3$							1.45×10^{-6}	14.5	20	-		
SiO_2	BTPA							8.70×10^{-7}	15	22	-		
F-induced SiO_2	TEFS	Sol-gel	α-Al_2O_3	300	750	300	-	1.50×10^{-6}	10.5	13	-	□	[114]
F-induced	BTESM+NH_4F	Sol-gel	α-Al_2O_3	900	350	200	200	9.50×10^{-7}	10.5	8.5	-	☆	[115]

SiO_2													
SiO_2	BTESE	Sol-gel	α-Al_2O_3	1000	300	200	-	1.60×10^{-7}	90	155	-		[116]
								1.50×10^{-6}	59	-	-		
	AHPCS				700			1.70×10^{-6}	10	7.5	-		
SiO_2+TiO_2	TiPCS				750			1.70×10^{-6}	5	4	-		
								2.10×10^{-8}	16	11.5	-		
SiO_2+Ta_2O_5	TEOS+TaEO	CVD	ZrO_2	20	650	400	0.015	1.48×10^{-8}	**11100**	**8200**	**4000**		This work
						500		2.46×10^{-8}	**12300**	**18200**	**2300**		
						650		1.40×10^{-7}	**5000**	**16000**	**640**		
								4.60×10^{-8}	**19000**	**26000**	**1700**		

AHPCS – Allylhydridopolycarbosilane;
APTES – (3-amino-propyl) triethoxysila;
APTMS – 3-aminopropyltrimethoxysilane;
ATSB – Aluminum-tri-sec-butoxide;
BTESA – Bis(triethox-ysilyl)acetylene;
BTESE – 1,2-bis(triethoxysilyl)ethane;
BTESEthy – 1,2-bis(triethoxysilyl)ethylene;
BTESM – Bis(triethoxysilyl)methane;
BTESP – Bis(triethoxysilyl)propane;
BTPA – Bis[3-(trimethoxysilyl)propyl] amine;
DES – Diethylsilane;
DMDMOS – Dimethyldimethoxysilane;
DMDPS – Dimethoxydiphenylsilane;
DPDES – Diphenyldiethoxysilane;
DPDMS – Diphenyldimethoxysilane;
HEDS – Hexaethoxy disiloxane;
HMDSO – Hexamethyldisiloxane;
HTMOS – Hexyltrimethoxysilane;
MAPTMS – (3-methylaminopropyl) trimethoxysilane;
MOTMS – Methacryloxypropyltrimethoxysilane;
MTMOS – Methyltrimetoxysilane;
MTES – Methyl-tri-ethoxy-silane;
NPB – Niobium(V) penta(n-butoxide);
PhTMOS – Phenyltrimethoxysilane;
POSS – Polyhedral oligomeric silsesquioxane;
PrTMOS – Propyltrimethoxysilane;
PTES – Phenyltriethoxysilane;
PTMS – Phenyltrimethoxysilane;
$SiAc_4$ – Silicon tetra-acetate;
TaEO – Tantalum (V) ethoxide;
TEFS –Triethoxyfluorosilane;
TEOS – Tetraethylorthosilicate;
TIP – Titanium isopropoxide;
TiPCS – Polytitanocarbosilane;
TIPT – Tetraisopropyl titanate;
TMOS – Tetramethoxysilane / Tetramethy orthosilicate;
TMMOS – Trimethylmethoxysilane;
TPMS – Triphenylmethoxysilane;
TPS – Triisopropylsilane;
TRIES – Triethoxysilane;
VTES – Vinyltriethoxysilane;
ZTB – Zirconium (IV) tert-butoxide;
ZTBO – Zirconium-n-butoxide;

Table S8. Summary of the selectivity and permeance for each membrane synthesized using the optimized boehmite sols and graded alumina structure technique.

Membrane No.	**Selectivity**			**Permeance** mol m^{-2} s^{-1} Pa^{-1}
	H_2/N_2	H_2/CH_4	H_2/O_2	H_2
1	340	2100	210	2.7×10^{-7}
1	600	2700	280	1.4×10^{-7}
2	5000	16000	640	1.4×10^{-7}
2	19000	26000	1700	4.6×10^{-8}
3	53	39	50	9.3×10^{-8}
4	1700	2100	720	1.0×10^{-7}
5	140	140	120	8.2×10^{-8}

Table S9. Summary of hydrothermal stability tests on silica-based porous membranes in the literature.

Membrane material	Precursor	Method	Support material	Pore size of support/ nm	Exposure time / h	H_2 permeance change / %	Final H_2 pemeance / mol s^{-1} m^{-2} Pa^{-1}	Temperature of hydrothermal stability test / ºC	Concentration of water vapor / mol %*	Symbol in Figs. 6 and S12	Ref.
SiO_2	TEOS	CVD	α-Al_2O_3	150	24	-37.5	1.84×10^{-9}	400	50		[19]
SiO_2+ZrO_2	TEOS+ZTBO	Sol-gel	α-Al_2O_3	1000	30	-17.5	2.80×10^{-6}	500	50		[39]
SiO_2+ZrO_2	TEOS+ZTBO	Sol-gel	α-Al_2O_3	1	30	-73	1.10×10^{-7}	500	13-33		[42]
SiO_2+NiO	TEOS+$Ni(NO_3)_2$	Sol-gel	α-Al_2O_3	1000	1680	-50	3.35×10^{-7}	40	4.4		[44]
SiO_2+Fe_2O_3	TEOS+$Fe(NO_3)_3$				840	-86.5	9.30×10^{-7}				
SiO_2	TEOM+O_2	CVD	α-Al_2O_3	-	82	-29	4.77×10^{-8}	500	75		[55]
SiO_2	TEOS	CVD	α-Al_2O_3	5	-	-60	4.00×10^{-8}	500	-	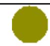	[56]
SiO_2	TEOS+O_2	CVD	α-Al_2O_3	100	80	-30	4.70×10^{-8}	500	75		[57]
SiO_2	TMMOS	CVD	α-Al_2O_3	100	58	-84	4.10×10^{-8}	600	75		[60]
	TMOS				80	-27	4.81×10^{-8}				
SiO_2+Co_3O_4	TEOS+$Co(NO_3)_2$	Sol-gel	α-Al_2O_3	1000	60	-50	4.00×10^{-8}	500	50	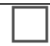	[67]
SiO_2+Al_2O_3	TEOS+ATSB	CVD	α-Al_2O_3	100	200	-39	1.28×10^{-7}	600	16		[69]
SiO_2	TEOS				100	-87	6.50×10^{-8}				
SiO_2+Nb_2O_5	TEOS+NPB	Sol-gel	α-Al_2O_3	-	70	-32	2.58×10^{-8}	200	56		[70]
SiO_2+TiO_2	TEOS+TIP	CVD	α-Al_2O_3	5	125	-30	9.10×10^{-8}	650	75		[72]
SiO_2+Co_3O_4	TEOS+ $Co(NO_3)_2$	Sol-gel	α-Al_2O_3	1000	60	-47	1.79×10^{-7}	500	30		[80]
SiO_2	TEOS+PTES	CVD	α-Al_2O_3	5	130	-50	2.20×10^{-7}	600	78		[84]
	TEOS				100	-87	6.50×10^{-8}		16		
SiO_2+ZrO_2	TEOS+ZTB	CVD	α-Al_2O_3	60	48	-56	1.72×10^{-7}	650	16		[96]

SiO_2+Al_2O_3	TEOS+ATSB	CVD	α-Al_2O_3	5	100	-45	3.85×10^{-8}	650	16	▼	[98]
					96	-68	2.27×10^{-8}				
SiO_2	VTES	CVD	α-Al_2O_3	60	48	-68	4.48×10^{-8}	600	16	●	[101]
					72	-55	2.32×10^{-7}				
F-induced SiO_2	TEFS	Sol-gel	α-Al_2O_3	500	15	-27	1.41×10^{-6}	300	30	▽	[102]
SiO_2	TEOS+TMMOS	CVD	α-Al_2O_3	60	96	-42	6.38×10^{-8}	650	16	◆	[106]
F-induced SiO_2	TEFS	Sol-gel	α-Al_2O_3	300	13	-93	3.00×10^{-8}	750	90	□	[114]
					29	-22	1.17×10^{-6}	500	30, 90		
					24	-33	1.46×10^{-6}	350	30, 90		
SiO_2+Ta_2O_5	TEOS+TaEO	CVD	ZrO_2	20	40	**-10.5**	4.12×10^{-8}	650	16	★	This study
					200	**-24.6**	3.47×10^{-8}				

* Note that partial pressure and mol % of H_2O are nearly identical as all experiments were performed under atmospheric pressure.

References

[1] G. Gavalas, C. Megiris, S. Nam, *Chem. Eng. Sci.* **1989**, 44, 1829.
[2] T. Okubo, H. Inoue, *AICHE J.* **1989**, 35, 845.
[3] G. R. Gavalas, C. E. Megiris (U.S. Patent), **1990**.
[4] M. Tsapatsis, S. Kim, G. Gavalas, S. W. Nam, *Ind. Eng. Chem. Res.* **1991**, 30, 2152.
[5] C. E. Megiris, J. H. Glezer, *Ind. Eng. Chem. Res.* **1992**, 31, 1293.
[6] G. R. Gavalas (California Inst. of Tech., Pasadena, CA (United States)) *U.S.*, **1992**.
[7] H. Y. Ha, S. W. Nam, W. K. Lee, *J. Membr. Sci.* **1993**, 85, 279.
[8] S. Yan, H. Maeda, K. Kusakabe, S. Morooka, Y. Akiyama, *Ind. Eng. Chem. Res.* **1994**, 33, 2096.
[9] M. Tsapatsis, G. Gavalas, *J. Membr. Sci.* **1994**, 87, 281.
[10] C. Lin, D. Flowers, P. Liu, *J. Membr. Sci.* **1994**, 92, 45.
[11] J. Wu, H. Sabol, G. Smith, D. Flowers, P. Liu, *J. Membr. Sci.* **1994**, 96, 275.
[12] R. De Lange, J. Hekkink, K. Keizer, A. Burggraaf, *Microporous Mater.* **1995**, 4, 169.
[13] R. De Lange, J. Hekkink, K. Keizer, A. Burggraaf, *J. Membr. Sci.* **1995**, 99, 57.
[14] S. Kim, G. R. Gavalas, *Ind. Eng. Chem. Res.* **1995**, 34, 168.
[15] S. Jiang, Y. Yan, G. Gavalas, *J. Membr. Sci.* **1995**, 103, 211.
[16] S. Morooka, S. Yan, K. Kusakabe, Y. Akiyama, *J. Membr. Sci.* **1995**, 101, 89.
[17] R. Levy, E. Ramos, L. Krasnoperov, A. Datta, J. Grow, *J. Mater. Res.* **1996**, 11, 3164.
[18] B.-K. Sea, M. Watanabe, K. Kusakabe, S. Morooka, S.-S. Kim, *Gas Sep. Purif.* **1996**, 10, 187.
[19] S. Morooka, S. Kim, S. Yan, K. Kusakabe, M. Watanabe, *Int. J. Hydrogen Energy* **1996**, 21, 183.
[20] H. H. Yong, J. S. Lee, S. W. Nam, I. W. Kim, S. A. Hong, *J. Mater. Sci. Lett.* **1997**, 16, 1023.
[21] B.-K. Sea, K. Kusakabe, S. Morooka, *J. Membr. Sci.* **1997**, 130, 41.
[22] R. M. De Vos, H. Verweij, *Science* **1998**, 279, 1710.
[23] A. Nijmeijer, B. Bladergroen, H. Verweij, *Microporous Mesoporous Mater.* **1998**, 25, 179.
[24] R. M. De Vos, H. Verweij, *J. Membr. Sci.* **1998**, 143, 37.
[25] S. Akiyama, H. Anzai, S. Morooka, H. Maeda, K. Kusakabe (Washington, DC: U.S. Patent and Trademark Office) *U.S.* , **1998**.
[26] B.-K. Sea, E. Soewito, M. Watanabe, K. Kusakabe, S. Morooka, S. S. Kim, *Ind. Eng. Chem. Res.* **1998**, 37, 2502.
[27] G.-J. Hwang, K. Onuki, S. Shimizu, H. Ohya, *J. Membr. Sci.* **1999**, 162, 83.
[28] R. M. De Vos, W. F. Maier, H. Verweij, *J. Membr. Sci.* **1999**, 158, 277.
[29] A. K. Prabhu, S. T. Oyama, *J. Membr. Sci.* **2000**, 176, 233.
[30] S.-I. Nakao, T. Suzuki, T. Sugawara, T. Tsuru, S. Kimura, *Microporous Mesoporous Mater.* **2000**, 37, 145.
[31] G. J. Hwang, K. Onuki, S. Shimizu, *AICHE J.* **2000**, 46, 92.

[32] C.-Y. Tsai, S.-Y. Tam, Y. Lu, C. J. Brinker, *J. Membr. Sci.* **2000**, 169, 255.
[33] B. Sea, K.-H. Lee, *J. Ind. Eng. Chem.* **2001**, 7, 417.
[34] S.-W. Nam, H.-Y. Ha, S.-P. Yoon, H. Jonghee, T.-H. Lim, I.-H. Oh, H. Seong-Ahn, *Korean Membrane J.* **2001**, 3, 69.
[35] K. Kuraoka, T. Kakitani, T. Suetsugu, T. Yazawa, *Sep. Purif. Technol.* **2001**, 25, 161.
[36] S.-S. Kim, B.-K. Sea, *Korean J. Chem. Eng.* **2001**, 18, 322.
[37] Y.-S. Kim, K. Kusakabe, S. Morooka, S.-M. Yang, *Korean J. Chem. Eng.* **2001**, 18, 106.
[38] B. G. Seo, G. H. Lee, *Bull. Korean Chem. Soc.* **2001**, 22, 1400.
[39] T. Tsuru, T. Tsuge, S. Kubota, K. Yoshida, T. Yoshioka, M. Asaeda, *Sep. Sci. Technol.* **2001**, 36, 3721.
[40] M. Asaeda, S. Yamasaki, *Sep. Purif. Technol.* **2001**, 25, 151.
[41] T. Yoshioka, E. Nakanishi, T. Tsuru, M. Asaeda, *AICHE J.* **2001**, 47, 2052.
[42] K. Yoshida, Y. Hirano, H. Fujii, T. Tsuru, M. Asaeda, *J. Chem. Eng. Japan* **2001**, 34, 523.
[43] D. Lee, S. T. Oyama, *J. Membr. Sci.* **2002**, 210, 291.
[44] M. Asaeda, M. Kanezashi, T. Yoshioka, T. Tsuru, *Mrs Proceedings* **2002**, 752.
[45] S. Giessler, L. Jordan, J. C. D. Costa, G. Q. M. Lu, *Sep. Purif. Technol.* **2003**, 32, 255.
[46] G. J. Hwang, J. W. Kim, H. S. Choi, K. Onuki, *J. Membr. Sci.* **2003**, 215, 293.
[47] K. Kusakabe, F. Shibao, G. Zhao, K. I. Sotowa, K. Watanabe, T. Saito, *J. Membr. Sci.* **2003**, 215, 321.
[48] D. L. A, L. Z. B, S. T. O. A, S. N. C, R. F. S. C *J. Membr. Sci.* **2004**, 231, 117.
[49] T. Zivkovic, N. E. Benes, D. Blank, H. Bouwmeester, *J. Sol-Gel Sci. Technol.* **2004**, 31, 205.
[50] T. Tsuru, K. Yamaguchi, T. Yoshioka, M. Asaeda, *AICHE J.* **2004**, 50, 2794.
[51] D. Lee, P. Hacarlioglu, S. T. Oyama, *Top. Catal.* **2004**, 29, 45.
[52] M. Nomura, K. Ono, S. Gopalakrishnan, T. Sugawara, S.-I. Nakao, *J. Membr. Sci.* **2005**, 251, 151.
[53] Y. Yoshino, T. Suzuki, B. N. Nair, H. Taguchi, N. Itoh, *J. Membr. Sci.* **2005**, 267, 8.
[54] M. Kanezashi, M. Asaeda, *J. Membr. Sci.* **2006**, 271, 86.
[55] M. Nomura, H. Aida, S. Gopatakrishnan, T. Sugawara, S.-I. Nakao, S. Yamazaki, T. Inada, Y. Iwamoto, *Desalination* **2006**, 193, 1.
[56] P. Hacarlioglu, Y. Gu, S. T. Oyama, *J. Nat. Gas Chem.* **2006**, 15, 73.
[57] S. Gopalakrishnan, M. Nomura, T. Sugawara, S. Nakao, *Desalination* **2006**, 193, 230.
[58] Y. Gu, S. T. Oyama, *Adv. Mater.* **2007**, 19, 1636.
[59] S. Gopalakrishnan, Y. Yoshino, M. Nomura, B. N. Nair, S. I. Nakao, *J. Membr. Sci.* **2007**, 297, 5.
[60] M. Nomura, T. Nagayo, K. Monma, *J. Chem. Eng. Japan* **2007**, 40, 1235.
[61] S. Araki, N. Mohri, Y. Yoshimitsu, Y. Miyake, *J. Membr. Sci.* **2007**, 290, 138.
[62] A. Brunetti, G. Barbieri, E. Drioli, K. H. Lee, B. Sea, D. W. Lee, *Chem. Eng.*

Process. **2007**, 46, 119.
[63] T. Nagano, S. Fujisaki, K. Sato, K. Hataya, Y. Iwamoto, M. Nomura, S.-I. Nakao, *J. Am. Ceram. Soc.* **2008**, 91, 71.
[64] K. Akamatsu, M. Nakane, T. Sugawara, T. Hattori, S.-I. Nakao, *J. Membr. Sci.* **2008**, 325, 16.
[65] Y. Ohta, K. Akamatsu, T. Sugawara, A. Nakao, A. Miyoshi, S.-I. Nakao, *J. Membr. Sci.* **2008**, 315, 93.
[66] S. Gopalakrishnan, J. C. D. da Costa, *J. Membr. Sci.* **2008**, 323, 144.
[67] R. Igi, T. Yoshioka, Y. H. Ikuhara, Y. Iwamoto, T. Tsuru, *J. Am. Ceram. Soc.* **2008**, 91, 2975.
[68] S. Battersby, M. C. Duke, S. M. Liu, V. Rudolph, J. C. D. da Costa, *J. Membr. Sci.* **2008**, 316, 46.
[69] Y. Gu, P. Hacarlioglu, S. T. Oyama, *J. Membr. Sci.* **2008**, 310, 28.
[70] V. Boffa, D. H. A. Blank, J. E. ten Elshof, *J. Membr. Sci.* **2008**, 319, 256.
[71] T. Tsuru, T. Morita, H. Shintani, T. Yoshioka, M. Asaeda, *J. Membr. Sci.* **2008**, 316, 53.
[72] Y. Gu, S. T. Oyama, *J. Membr. Sci.* **2009**, 345, 267.
[73] M. Kanezashi, K. Yada, T. Yoshioka, T. Tsuru, *J. Am. Chem. Soc.* **2009**, 131, 414.
[74] D. Koutsonikolas, S. Kaldis, G. P. Sakellaropoulos, *J. Membr. Sci.* **2009**, 342, 131.
[75] M. Kanezashi, K. Yada, T. Yoshioka, T. Tsuru, *J. Membr. Sci.* **2010**, 348, 310.
[76] D. E. Koutsonikolas, S. P. Kaldis, S. D. Sklari, G. Pantoleontos, V. T. Zaspalis, G. P. Sakellaropoulos, *Microporous Mesoporous Mater.* **2010**, 132, 276.
[77] H. Lim, Y. F. Gu, S. T. Oyama, *J. Membr. Sci.* **2010**, 351, 149.
[78] M. W. J. Luiten, N. E. Benes, C. Huiskes, H. Kruidhof, A. Nijmeijer, *J. Membr. Sci.* **2010**, 348, 1.
[79] T. Tsuru, H. Shigemoto, M. Kanezashi, T. Yoshioka, *Chem. Commun.* **2011**, 47, 8070.
[80] T. Tsuru, R. Igi, M. Kanezashi, T. Yoshioka, S. Fujisaki, Y. Iwamoto, *AICHE J.* **2011**, 57, 618.
[81] H. R. Lee, T. Shibata, M. Kanezashi, T. Mizumo, J. Ohshita, T. Tsuru, *J. Membr. Sci.* **2011**, 383, 152.
[82] M. Amanipour, E. G. Babakhani, A. Safekordi, A. Zamaniyan, M. Heidari, *J. Membr. Sci.* **2012**, 423, 530.
[83] C. Yacou, S. Smart, J. D. Costa, *Energy Environ. Sci.* **2012**, 5, 5820.
[84] Y. Gu, Vaezian, B., Khatib, S. J., Oyama, S. T., Wang, Z., Achenie, L. , *Sep. Sci. Technol.* **2012**, 47, p.1698.
[85] M. Kanezashi, M. Kawano, T. Yoshioka, T. Tsuru, *Ind. Eng. Chem. Res.* **2012**, 51, 944.
[86] M. Kanezashi, W. N. Shazwani, T. Yoshioka, T. Tsuru, *J. Membr. Sci.* **2012**, 415, 478.
[87] H. H. Han, S. H. Ryu, S.-i. Nakao, Y. T. Lee, *J. Membr. Sci.* **2013**, 431, 72.
[88] M. Nomura, Y. Nishi, T. Sakanishi, K. Utsumi, R. Nakamura, *Energy Procedia*

2013, 37, 1012.
[89] E. Matsuyama, A. Ikeda, M. Komatsuzaki, M. Sasaki, M. Nomura, *Sep. Purif. Technol.* **2014**, 128, 25.
[90] R. Xu, S. M. Ibrahim, M. Kanezashi, T. Yoshioka, K. Ito, J. Ohshita, T. Tsuru, *ACS Appl. Mater. Inter.* **2014**, 6, 9357.
[91] A. Jabbari, K. Ghasemzadeh, P. Khajavi, F. Assa, M. Abdi, A. Babaluo, A. Basile, *Int. J. Hydrogen Energy* **2014**, 39, 18585.
[92] K. Ghasemzadeh, A. Aghaeinejad-Meybodi, M. J. Vaezi, A. Gholizadeh, M. A. Abdi, A. A. Babaluo, M. Haghighi, A. Basile, *RSC Adv.* **2015**, 5, 95823.
[93] H. Nagasawa, T. Minamizawa, M. Kanezashi, T. Yoshioka, T. Tsuru, *J. Membr. Sci.* **2015**, 489, 11.
[94] S. B. Messaoud, A. Takagaki, T. Sugawara, R. Kikuchi, S. T. Oyama, *J. Membr. Sci.* **2015**, 477, 161.
[95] X. L. Zhang, H. Yamada, T. Saito, T. Kai, K. Murakami, M. Nakashima, J. Ohshita, K. Akamatsu, S. Nakao, *J. Membr. Sci.* **2016**, 499, 28.
[96] S.-J. Ahn, A. Takagaki, T. Sugawara, R. Kikuchi, S. T. Oyama, *J. Membr. Sci.* **2017**, 526, 409.
[97] O. Myagmarjav, A. Ikeda, N. Tanaka, S. Kubo, M. Nomura, *Int. J. Hydrogen Energy* **2017**, 42, 6012.
[98] N. Kageyama, A. Takagaki, T. Sugawara, R. Kikuchi, S. T. Oyama, *Sep. Purif. Technol.* **2018**, 195, 437.
[99] N. Moriyama, H. Nagasawa, M. Kanezashi, K. Ito, T. Tsuru, *J. Sol-Gel Sci. Technol.* **2018**, 86, 63.
[100] S. J. Ahn, G. N. Yun, A. Takagaki, R. Kikuchi, S. T. Oyama, *Sep. Purif. Technol.* **2018**, 194, 197.
[101] S. J. Ahn, G. N. Yun, A. Takagaki, R. Kikuchi, S. T. Oyama, *J. Membr. Sci.* **2018**, 550, 1.
[102] M. Kanezashi, T. Matsutani, H. Nagasawa, T. Tsuru, *J. Membr. Sci.* **2018**, 549, 111.
[103] N. Moriyama, H. Nagasawa, M. Kanezashi, T. Tsuru, *Sep. Purif. Technol.* **2018**, 207, 108.
[104] T. Tanaka, M. Kanezashi, H. Nagasawa, T. Tsuru, *Ind. Eng. Chem. Res.* **2019**, 58, 3867.
[105] M. Kanezashi, Y. Tomarino, H. Nagasawa, T. Tsuru, *J. Membr. Sci.* **2019**, 582, 59.
[106] Y. Mise, S. J. Ahn, A. Takagaki, R. Kikuchi, S. T. Oyama, *Membranes* **2019**, 9.
[107] H. Nagasawa, T. Kagawa, T. Noborio, M. Kanezashi, A. Ogata, T. Tsuru, *J. Am. Chem. Soc.* **2020**, 143, 35.
[108] S. Lawal, M. Kanezashi, H. Nagasawa, T. Tsuru, *J. Membr. Sci.* **2020**, 599, 117844.
[109] R. Inoue, M. Kanezashi, H. Nagasawa, K. Yamamoto, T. Gunji, T. Tsuru, *Sep. Purif. Technol.* **2020**, 242, 116742.
[110] M. Guo, M. Kanezashi, H. Nagasawa, L. Yu, J. Ohshita, T. Tsuru, *J. Membr. Sci.* **2020**, 611, 118328.

[111] S. O. Lawal, H. Nagasawa, T. Tsuru, M. Kanezashi, *Molecular Systems Design & Engineering* **2021**, 6, 429.
[112] K. Nakahiro, L. Yu, H. Nagasawa, T. Tsuru, M. Kanezashi, *Ind. Eng. Chem. Res.* **2021**.
[113] U. Anggarini, L. Yu, H. Nagasawa, M. Kanezashi, T. Tsuru, *Materials Chemistry Frontiers* **2021**, 5, 3029.
[114] M. Kanezashi, N. Hataoka, R. Ikram, H. Nagasawa, T. Tsuru, *AICHE J.* **2021**.
[115] M. Takenaka, H. Nagasawa, T. Tsuru, M. Kanezashi, *J. Membr. Sci.* **2021**, 619, 118787.
[116] N. Moriyama, Y. Kawano, Q. Wang, R. Inoue, M. Guo, M. Yokoji, H. Nagasawa, M. Kanezashi, T. Tsuru, *AICHE J.* **2021**, 67, e17223.